ATLAS PUB Note
ATL-PHYS-PUB-2025-014
26th March 2025

Updated projections for Higgs boson measurements using $H \to \gamma\gamma$, $Z\gamma$, $\mu\mu$ decays and for the combined measurement of Higgs boson couplings with the ATLAS detector at the HL-LHC

The ATLAS Collaboration

Updated estimates are presented of the expected precision for the Higgs boson measurements in the $H \to \gamma\gamma$, $Z\gamma$ and $\mu\mu$ final states with the ATLAS detector at the High Luminosity LHC. The measurements performed in the same final states using the full ATLAS Run 2 data are projected to integrated luminosities ranging from 1000 fb^{-1} to 3000 fb^{-1}, at a centre-of-mass energy of 14 TeV. They are obtained in baseline, optimistic and conservative scenarios of systematic uncertainties. In addition, the latest ATLAS extrapolations of single Higgs-boson measurements in the baseline uncertainty scenario with 3000 fb^{-1} are used in a joint interpretation to derive the expected uncertainties in the scale factors of various Higgs boson coupling strengths.

Contents

1 Introduction

The elucidation of the mechanism of spontaneous electroweak symmetry breaking and of mass generation of the elementary matter particles is one of the highest priorities in future particle physics collider projects. An unparalleled investigation into these phenomena will be enabled by the high-luminosity upgrade of the LHC (HL-LHC), via unprecedentedly precise and comprehensive measurements of the Higgs boson properties [1].

The precision of measurements of Higgs boson production cross section times branching ratios and Higgs boson couplings at the HL-LHC was estimated by the ATLAS Collaboration in late 2018 [2]. An integrated luminosity of 3000 fb^{-1} of pp collisions at a centre-of-mass energy $\sqrt{s}$ = 14 TeV collected by the upgraded ATLAS detector and passing data-quality requirements was assumed. The study combined a comprehensive set of final states and event categories to target the five main Higgs boson production modes and seven of its decays. Expected constraints on nine modifiers κ that act as scale factors of the Higgs boson coupling strengths to other Standard Model (SM) particles and branching ratio to beyond-SM (BSM) final states were also derived. The results were based on the extrapolation of the sensitivities of analyses performed on partial Run 2 ATLAS datasets, corresponding to integrated luminosities of 36 fb^{-1} or 80 fb^{-1}.

The sensitivities of the analyses of the full Run 2 ATLAS dataset (140 fb^{-1} of pp collisions) performed more recently than the extrapolations of Ref. [2], generally exceed those expected from a simple scaling for the larger event samples. This effect has multiple origins, including better understanding of detector performance, improved analysis techniques, and more granular analysis regions with better signal-to-noise ratio accessible with the larger dataset.

This note provides updated estimates on the expected precision of the measurements of the Higgs boson cross sections times branching ratios at the HL-LHC with the ATLAS detector for a selected subset of final

states. It focuses on decays that are rare in the Standard Model, but have a clean experimental signature, $H \to \gamma\gamma$, $Z\gamma$, $\mu\mu$, as those benefit the most from the increase of integrated luminosity of about one order of magnitude from LHC to HL-LHC. The results are then combined with the latest ATLAS extrapolations of other single-Higgs boson measurements, either from Ref. [2] or from updated projections for VH, $H \to b\bar{b}$ and $H \to c\bar{c}$ [3] and $H \to \tau\tau$ [4], to estimate the expected constraints on several scale factors of Higgs boson coupling strengths, in the baseline uncertainty scenario for 3000 fb^{-1}.

2 Extrapolation procedure

The methodology is similar to the one outlined in Ref. [2] and briefly summarised here. The performance of the upgraded ATLAS detector in the harsher pile-up environment of the HL-LHC is expected to match that of the current detector during the LHC Run 2. This hypothesis is supported by detector performance studies documented in Refs. [5, 6]. A notable exception is the muon momentum resolution: the new ATLAS Inner Tracker (ITk) [7] and the upgraded muon spectrometre at HL-LHC will provide a significantly more precise determination of the muon momentum than the current detector [5]. This effect has been taken into account in the extrapolations of the $H \to \mu\mu$ analysis, which benefits the most from this improvement.

For simplicity, the same analysis strategies employed in the full Run 2 measurements are assumed to be used for the analysis of the HL-LHC dataset. In particular, event selection, classification, modelling of signal and backgrounds, and determination of signal and background yields through maximum likelihood fits to distributions of observable quantities in data, are supposed to be the same. Under these assumptions, extrapolations are be obtained by fitting the expected signal and background distributions determined by the Run 2 data analyses, after a rescaling that accounts for the larger cross sections and integrated luminosity of the HL-LHC. Future improvements are likely due to advanced analysis techniques or better sensitivities from tighter event selections with larger signal-to-background ratio, and therefore these estimates should be considered as conservative.

The HL-LHC centre-of-mass energy of the colliding protons is assumed to be $\sqrt{s} = 14$ TeV. The signal and background distributions predicted by the Run 2 analyses are thus scaled by the ratios of their cross sections at 14 and 13 TeV [8], as summarised in Table 1. Signal production modes include gluon–gluon fusion (ggF), vector-boson fusion (VBF), associated production with a W (WH) or Z (ZH) boson, with a top or bottom quark-antiquark pair ($t\bar{t}H$, $b\bar{b}H$), or with a single top quark or antiquark (tH). Different scaling factors are used for backgrounds produced mainly by gg or qq elementary interactions [9]. The dependence of the sensitivity to these scaling factors is small.

The results for single-channel measurements are presented for the nominal value of the integrated luminosity for a single HL-LHC experiment, 3000 fb^{-1}, as well as for more conservative values (1000 fb^{-1} and 2000 fb^{-1}) corresponding to early analyses of partial datasets.

Three scenarios are considered for the experimental and theoretical systematic uncertainties affecting the measurements:

- *Run 2 systematic uncertainties*: a conservative scenario where all the systematic uncertainties are assumed to be of the same size as in the published Run 2 analyses;
- *baseline systematic uncertainties*: the reference scenario, in which: (i) uncertainties related to background modelling, i.e. spurious signals [10–12], and also the uncertainties arising from limited MC statistics are negligible; (ii) all the theoretical systematic uncertainties as well as the experimental

Table 1: Cross section scaling factors from $\sqrt{s}$ = 13 TeV to $\sqrt{s}$ = 14 TeV for signal and background processes used in this study, assuming a Higgs boson mass of 125.09 GeV [8, 9].

Process	Scale factor
ggF	1.13
VBF	1.13
WH	1.10
ZH	1.11
$t\bar{t}H$	1.21
$b\bar{b}H$	1.14
tH	1.21
background (gg-initiated)	1.12
background (qq-initiated)	1.08

systematic uncertainties in the calibration of the flavour tagging efficiency of b- and c-jets are halved with respect to those of the Run 2 analyses; (iii) uncertainties in photon identification and isolation efficiency are reduced by 20%; (iv) all other experimental systematic uncertainties are as in the latest published results. This scenario is based on the studies [5, 6] and discussions with the theory community and the CMS Collaboration for sensitivity projections performed in the context of the 2019 Update of the European Strategy for Particle Physics Ref. [2] and of the 2022 Snowmass process [13].

- *no systematic uncertainties*: an optimistic scenario where all systematic uncertainties are considered to be negligible compared to statistical ones. This shows the ultimate precision that could be reached in the ideal case of extremely accurate theoretical calculations and detector calibrations (with the caveat underlined previously that the projections do not take into account potential improvements in analysis techniques).

The three scenarios are summarised in Table 2. Scenarios similar to the first two were considered also in Ref. [2], where they are denoted S1 and S2, respectively.

Table 2: Scaling factor for the systematic uncertainties used in the extrapolations, with respect to the full Run 2 analyses.

Uncertainty source	Uncertainty scale factor		
	Run 2 systematic uncertainties	Baseline	No systematic uncertainties
Background modelling uncertainties	1.0	0.0	0.0
MC statistical uncertainties	1.0	0.0	0.0
Photon identification and isolation	1.0	0.8	0.0
Flavour tagging of b, c jets	1.0	0.5	0.0
Other experimental systematic uncertainties	1.0	1.0	0.0
Theoretical uncertainties	1.0	0.5	0.0

Results on the coupling strength scale factors quoted in this note are obtained using the κ-framework [9]. In this approach, the rates of various Higgs boson production and decay modes (labeled i and f, respectively)

are expressed under the narrow-width assumption as

$$\sigma_i \times \mathcal{B}(H \to f) = \frac{\sigma_i \Gamma_f}{\Gamma_H} = \frac{\kappa_i^2 \kappa_f^2}{\kappa_H^2} \sigma_i^{\mathrm{SM}} \times \mathcal{B}^{\mathrm{SM}}(H \to f)$$

where κ_i and κ_f are the multiplicative coupling strength scale factors applied to the SM Higgs boson production cross section (σ_i^{SM}) and decay branching ratio ($\mathcal{B}^{\mathrm{SM}}(H \to f)$), respectively, and κ_H is the scale factor for the total width of the Higgs boson. Throughout this note, it is assumed that the Higgs boson couples only to Standard Model particles and its width scale factors κ_H can thus be expressed as a function of the other coupling strength scale factors.

3 Results

3.1 $H \to \gamma\gamma$

The Run 2 $H \to \gamma\gamma$ measurement [10] provides good sensitivity to all major Higgs boson production modes at the LHC, with the exception of associated $b\bar{b}H$ production. This mode was not targeted as it exhibits kinematic properties similar to those of gluon-gluon fusion but has a cross section approximately two orders of magnitude smaller. The uncertainties of the published results of Ref. [10] are updated for this extrapolation to take into account improved determinations of the total integrated luminosity (0.83% instead of 1.7%) [14] and of the photon energy scale (more than twice as precise as the previous calibration) [15]; the Higgs boson mass uncertainty (±240 MeV in Ref. [10]) is expected to be below 50 MeV [2], with a negligible impact on these results, and thus not included in this projection study.

The expected precision of various measurements of production-mode cross section times the branching ratio of the $H \to \gamma\gamma$ decay, $\mathcal{B}(H \to \gamma\gamma)$, as functions of the integrated luminosity and for the different uncertainty scenarios, is shown in Figure 1. The decomposition of the total uncertainty into statistical and systematic components is shown in Appendix A. Compared with the measurement used in the previous projection studies [2], the updated $H \to \gamma\gamma$ analysis is able to simultaneously constrain the cross sections of WH and ZH modes. It also provides a measurement of the tH production cross section with about 50% relative uncertainty in the baseline scenario, in which sources of systematic uncertainties that were estimated in a conservative way in the Run 2 analysis are assumed to be significantly reduced. With respect to Ref. [2], the projected uncertainty in the ggF production cross section is similar, but there are substantial improvements in other modes – between 15 and 27% – when considering the same set of parameters of interest, as shown in Appendix A.

The updated $H \to \gamma\gamma$ measurement also provides differential cross section measurements for each production mode within the Simplified Template Cross Section (STXS) framework [16]. The projected sensitivity to 33 simplified template cross sections times $\mathcal{B}(H \to \gamma\gamma)$ with an integrated luminosity of 3000 fb^{-1} in the three uncertainty scenarios under study is shown in Figure 2. Compared to the Run 2 analysis [10], a finer granularity STXS measurement is presented in this note to reflect larger HL-LHC dataset.

The expected contraints on the effective coupling strength scale factors for Higgs-photon (κ_γ) and Higgs-gluon (κ_g) interactions are shown in Figure 3, with other coupling strength scale factors fixed to their SM values of unity. These loop-induced couplings are sensitive to physics beyond the SM (BSM). The different

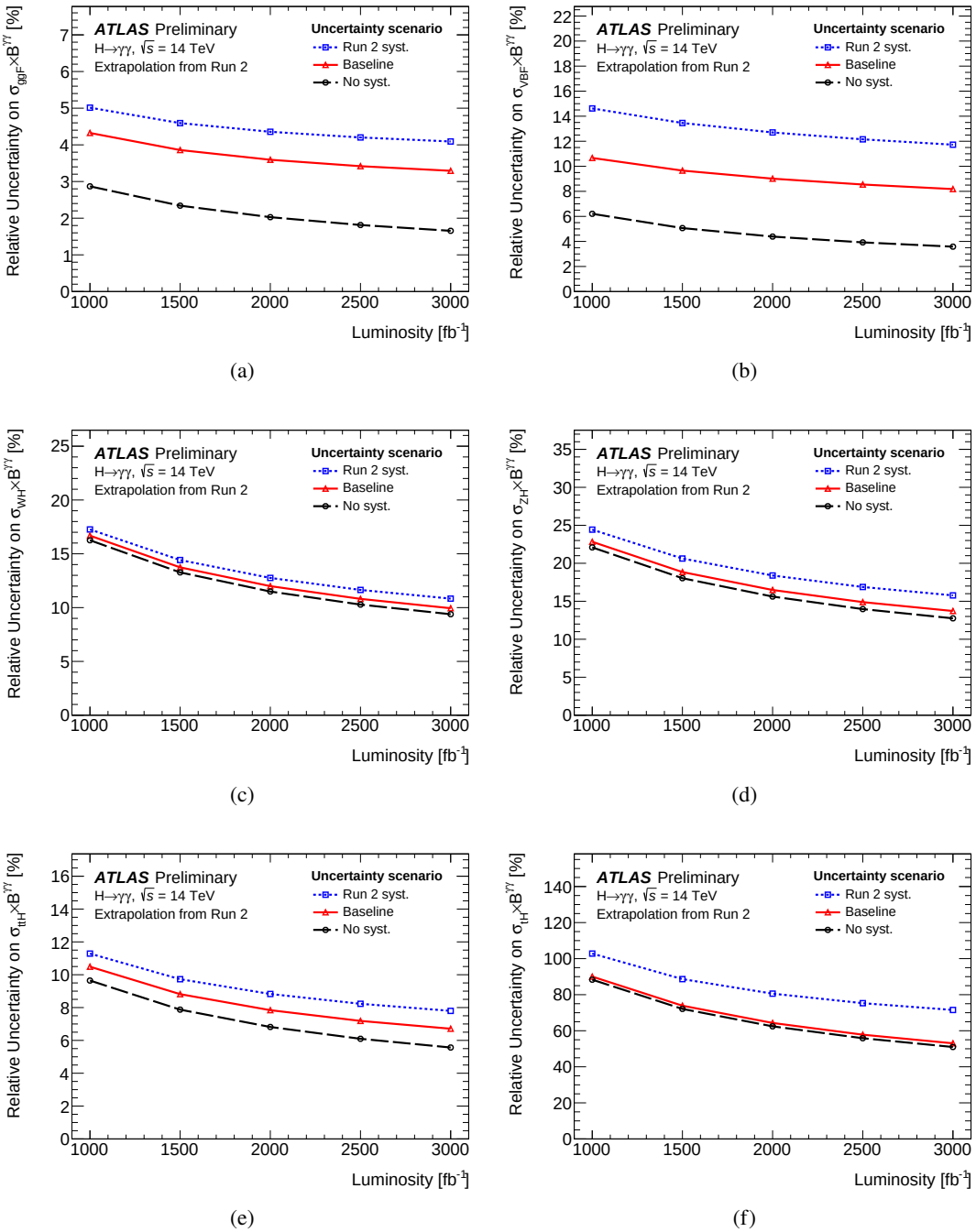

Figure 1: The projected uncertainties on the cross sections of SM (a) ggF, (b) VBF, (c) WH, (d) ZH, (e) $t\bar{t}H$, and (f) tH processes measured in the $H \to \gamma\gamma$ channel by the ATLAS experiment for integrated luminosities between 1000 and 3000 fb^{-1}. Three systematic uncertainty scenarios as defined in the text, namely *Run 2*, *baseline*, and *no systematic uncertainties*, have been considered.

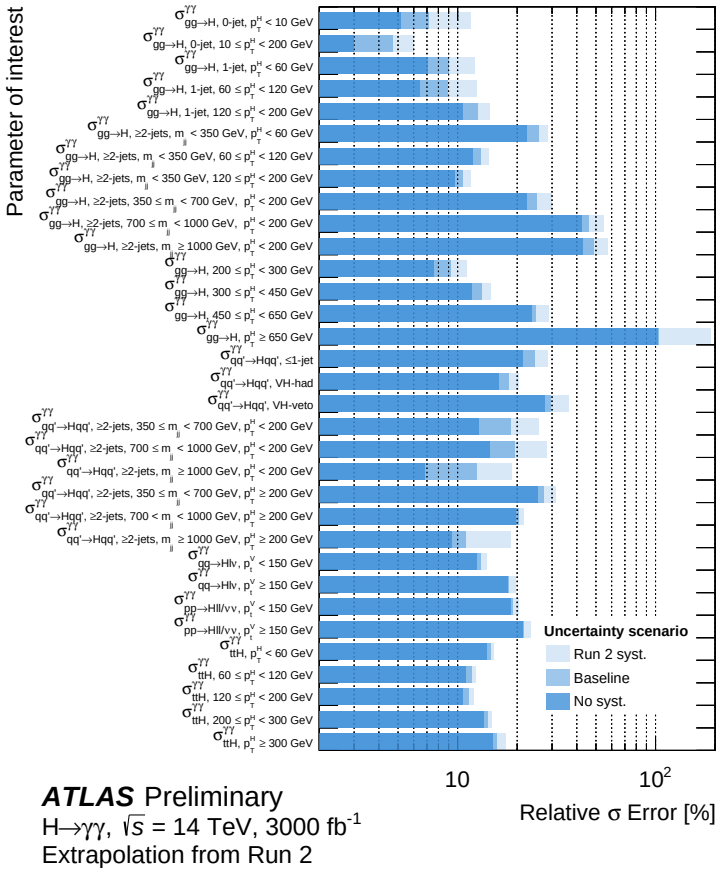

Figure 2: The projected uncertainty in 33 simplified template cross sections times $\mathcal{B}(H \to \gamma\gamma)$ with 3000 fb^{-1} of pp collisions for three different uncertainty scenarios.

orientations of the confidence regions when systematic uncertainties are included or not in Fig. 3(a) arise from signal modelling uncertainties.

The projected sensitivity to constrain the scaling factor for the Higgs-top Yukawa coupling strength κ_t is shown in Figure 4, either using only the tree-level constraint provided by the $t\bar{t}H$ and tH production modes, or also including contributions from loop-induced ggF and $H \to \gamma\gamma$ decay. In the latter case, the loop-induced Higgs boson couplings to the gluon and the photon are resolved in terms of the contributions from other SM particles. These constraints on the coupling strength scale factors are all provided with a single decay channel, with other coupling strength scale factors set to unity.

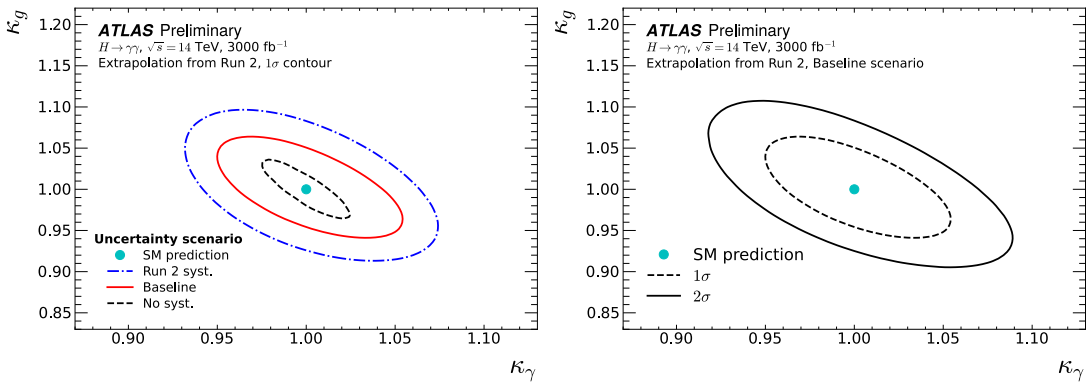

(a) (b)

Figure 3: The projected two-dimensional confidence regions of the coupling strength scale factors κ_g vs κ_γ for (a) the three uncertainty scenarios, at 68% C.L., and for (b) the *baseline* uncertainty scenario, at both 68% and 95% C.L., measured in the $H \to \gamma\gamma$ channel by the ATLAS experiment with an integrated luminosity of 3000 fb^{-1}. Other coupling strength scale factors are fixed at SM values.

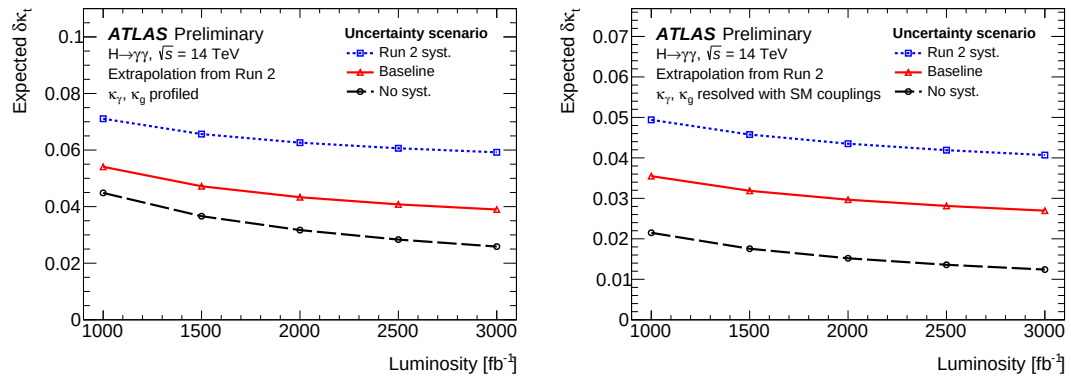

(a) (b)

Figure 4: The projected uncertainty in the top-Higgs Yukawa coupling strength scale factor κ_t measured in the $H \to \gamma\gamma$ channel by the ATLAS experiment for integrated luminosities between 1000 and 3000 fb^{-1}. The measurement is performed either (a) using only tree-level constraint provided by the $t\bar{t}H$ and tH production modes, or (b) also including loop-induced constraints from ggF and $H \to \gamma\gamma$. Other coupling strength scale factors are fixed at SM values. Three systematic uncertainty scenarios as defined in the text, namely *Run 2*, *baseline*, and *no systematic uncertainties*, have been considered.

3.2 $H \to Z\gamma$

The $H \to Z\gamma$ decay channel has a small branching ratio in the SM: $\mathcal{B}(H \to Z\gamma) = (1.5 \pm 0.1) \times 10^{-3}$ [8]. The most sensitive measurements of this process proceed through the reconstruction of Z boson decays to electron-positron or muon-antimuon pairs, whose branching ratio is only 6.7%, leading to an overall Higgs boson branching ratio $\mathcal{B}(H \to Z\gamma \to \ell\ell\gamma) \approx 10^{-4}$ ($\ell = e, \mu$). The photon and leptons from the $H \to Z\gamma \to \ell\ell\gamma$ decay are produced with low transverse momenta, making it difficult to efficiently reconstruct these final states with good background discrimination. For these reasons, the measurement of the $H \to Z\gamma$ signal strength and the corresponding scale factor of the effective coupling strength ($\kappa_{Z\gamma}$) is dominated by statistical uncertainties. Recently, evidence for the $H \to Z\gamma$ decay with a significance of three standard deviations was obtained by a joint interpretation of searches performed by ATLAS and CMS with their full Run 2 datasets [17] (total luminosity of about 280 fb^{-1}); a signal strength $\mu = 2.2 \pm 0.7$ was measured.

The extrapolations shown in this document are based on the published ATLAS Run 2 analysis [11]. The

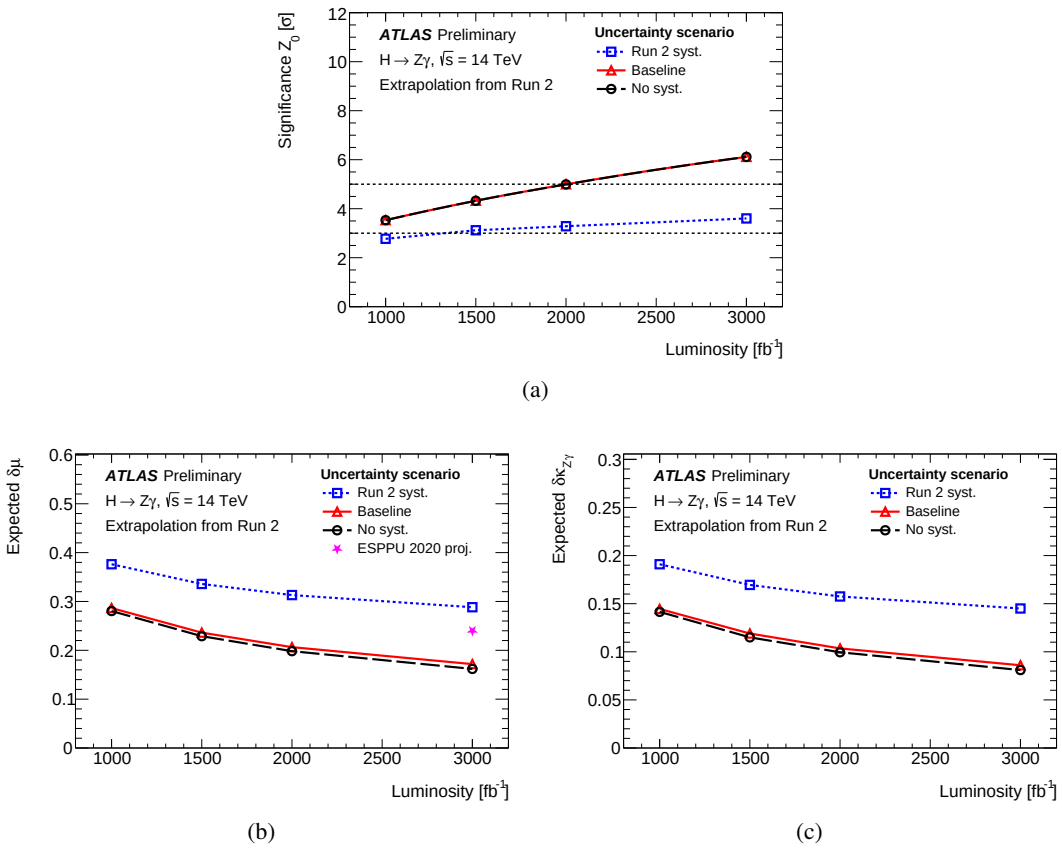

Figure 5: The projected (a) significance Z_0, (b) signal strength uncertainty $\delta\mu$, and (c) coupling strength scale factor uncertainty $\delta\kappa_{Z\gamma}$ of a SM $H \to Z\gamma$ signal measured by the ATLAS experiment with integrated luminosities between 1000 and 3000 fb^{-1}. Three systematic uncertainty scenarios as defined in the text, namely *Run 2* (blue open squares), *baseline* (red open triangles), and *no systematic uncertainties* (black open circles), have been considered. The prediction of the previous projection prepared for European Strategy for Particle Physics Update in 2020 (ESPPU 2020) [2] in a scenario (S2) similar to the *baseline* one for an integrated luminosity of 3000 fb^{-1} is also shown (magenta star).

statistical significance expected at the HL-LHC for this process in the SM hypothesis ($\mu = 1$) for integrated luminosities between 1000 and 3000 fb^{-1} is shown in Figure 5(a). In the *Run 2* uncertainties scenario, observation with more than five standard deviations of this process would be precluded by the large background modelling uncertainty conservatively assigned in the Run 2 measurement. In the other two scenarios, where this uncertainty is assumed to be negligible, a 5σ observation could be achieved already by a single experiment with 2000 fb^{-1}. As systematic uncertainties in the *baseline* scenario affect mainly the signal, discovery significance Z_0 is similar between *baseline* and *no systematic uncertainties* scenarios.

The expected uncertainties on the signal strength and on the effective coupling strength scale factor $\kappa_{Z\gamma}$ as a function of the integrated luminosity for the various uncertainty scenarios are shown in Figure 5(b) and 5(c), respectively. The loop-induced $\kappa_{Z\gamma}$ coupling strength is not resolved in terms of the contributions from other SM particles, and all other coupling strengths are fixed to their SM values of unity. In the *baseline* scenario, the uncertainty on the signal strength ($\kappa_{Z\gamma}$) would decrease from 21% to 17% (10% to 8%) between 2000 and 3000 fb^{-1}

In the *Run 2* uncertainty scenario, the precision on the signal strength and $\kappa_{Z\gamma}$ would be significantly degraded due to the background modeling uncertainties, while in the optimistic scenario of *no systematic uncertainties* it would be improved by only a few percent with respect to *baseline*, indicating that the role played by other systematic uncertainties excluding the background modelling ones is minor compared to the statistical uncertainty.

These updated projections demonstrate a much improved sensitivity compared to the previous extrapolation [2] from the 36 fb^{-1} ATLAS Run 2 analysis [18], which predicted a significance of 4.9 standard deviations and an uncertainty in the signal strength of 24% with 3000 fb^{-1} of data in an uncertainty scenario (S2) similar to the baseline one. The improvement is mainly from the improved analysis techniques introduced in the analysis based on full Run 2 dataset [11].

3.3 $H \to \mu\mu$

The $H \to \mu\mu$ channel is unique in testing the origin of mass of second generation of fermions. The smallness of its branching ratio (2×10^{-4}), combined with the large background from Drell-Yan di-muon production, results in a signal-over-background ratio at the per-mil level.

The projection reported in this note is based on the search for $H \to \mu\mu$ decays based on full ATLAS Run 2 dataset [12]. Compared with the input search used in Ref. [2], improvements in several aspects of the analysis techniques, including better muon reconstruction, machine-learning-based dataset categorisation, and consolidated background modeling, lead to 25% improvement in the sensitivity. A $2.0\,\sigma$ excess compatible with $H \to \mu\mu$ signal was observed in the Run 2 data, with a signal strength of $\mu = 1.2 \pm 0.6$.

The resolution of the muon momentum measurement is of paramount importance to the measurement of $H \to \mu\mu$ signal, as it determines the signal-over-background ratio. In order to account for expected improvements in the muon momentum resolution brought by the ITk, the resolution of the Higgs boson peak is reduced by 30% in VBF and 0-jet categories, and 15% in other categories, following a similar strategy adopted by Ref. [2].

The statistical significance expected at the HL-LHC for this process in the SM hypothesis ($\mu = 1$) for integrated luminosities between 1000 and 3000 fb^{-1} is shown in Figure 6(a). In all scenarios considered the signal would be observed with significance greater than five standard deviations. In the *baseline* scenario, the expected significance is greater than 10σ (6σ) with 3000 (1000) fb^{-1}.

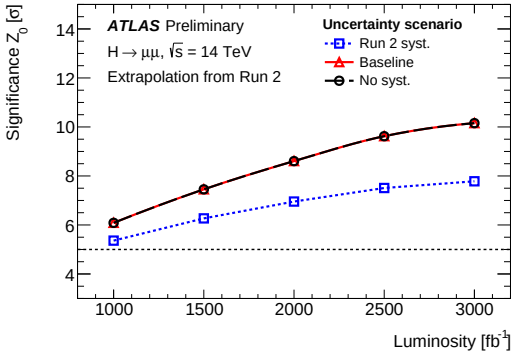

(a)

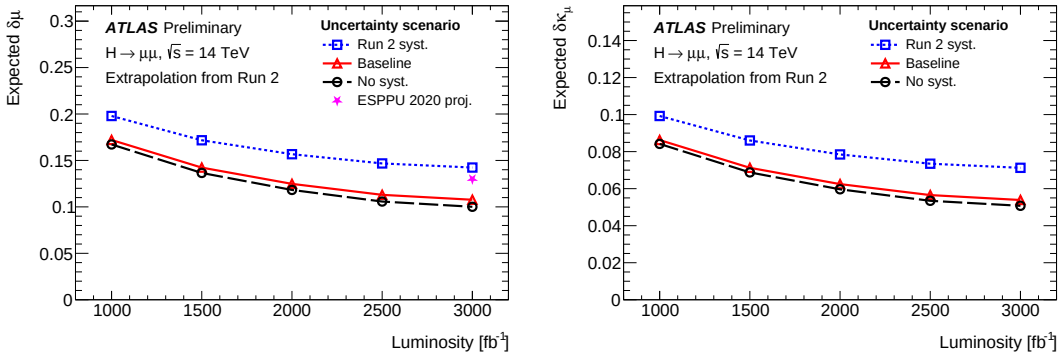

(b) (c)

Figure 6: The projected (a) significance Z_0, (b) signal strength uncertainty $\delta\mu$, and (c) coupling strength scale factor uncertainty $\delta\kappa_\mu$ of a SM $H \to \mu\mu$ signal measured by the ATLAS experiment with integrated luminosities between 1000 and 3000 fb^{-1}. Three systematic uncertainty scenarios as defined in the text, namely *Run 2* (blue open squares), *baseline* (red open triangles), and *no systematic uncertainties* (black open circles), have been considered. The prediction of the previous projection prepared for European Strategy for Particle Physics Update in 2020 (ESPPU 2020) [2] in a scenario (S2) similar to the *baseline* one for an integrated luminosity of 3000 fb^{-1} is also shown (magenta star).

The expected precision results on the signal strength and the muon Yukawa coupling strength scale factor κ_μ (with all other coupling strength scale factors fixed to unity) as a function of the integrated luminosity for the various uncertainty scenarios are shown in Figure 6(b) and 6(c), respectively. In the *baseline* scenario, the signal strength (muon coupling strength scale factor) uncertainty would decrease from 13% to 11% (6.5% to 5.4%) between 2000 and 3000 fb^{-1}. For comparison, the previous extrapolation [2] from a search for $H \to \mu\mu$ decays with 80 fb^{-1} of ATLAS Run 2 data [19] predicted an uncertainty in the signal strength of 13% with 3000 fb^{-1} of data in an uncertainty scenario (S2) similar to the *baseline* one.

3.4 Combination

The projected sensitivity of a combined measurement of Higgs boson couplings within the κ-framework, previously reported in Ref. [2], is updated using the latest extrapolations for the measurements of $H \to \gamma\gamma$, $H \to \mu\mu$, and $H \to Z\gamma$ (this document), of VH, $H \to b\bar{b}$ [3], and of $H \to \tau\tau$ [4]. Only the *baseline* systematic uncertainty scenario is considered for above projections. For other Higgs boson production and

decay processes, the projections of Ref. [2] are used, considering only the "S2" scenario as defined in the reference. An integrated luminosity of 3000 fb^{-1} is assumed for this study. The inputs are summarised in Table 3.

The correlation of the following systematic uncertainty sources is considered among all the input projection measurements: luminosity, pile-up, QCD uncertainty in Higgs boson production cross sections, parton distribution functions, Higgs boson decay branching ratio, and parton shower. In addition, the uncertainties in jet, missing transverse momentum, electron, photon, and muon reconstruction and calibration are correlated where possible between the updated projections and unmodified ones from Ref. [2]. The correlation of systematic uncertainties among the unmodified projections remain unchanged with respect to Ref. [2].

Table 3: Summary of input projection measurements for the combined projection study. The processes targeted by each input is broken down into production and decay modes (first and second columns, respectively). The third column provides the reference for the extrapolation, while the fourth gives the integrated luminosity used by the measurement on which the extrapolation is based. For comparison, the last column shows the integrated luminosities of the measurements used in the previous extrapolations documented in Ref. [4].

Production	Decay	Reference	$\mathcal{L}$ of projected measurement [fb^{-1}]	
			this study	previous study [4]
ggF, VBF, WH, ZH, $t\bar{t}H$, tH	$H \to \gamma\gamma$	Sec. 3.1	140	80
ggF, VBF	$H \to Z\gamma$	Sec. 3.2	140	36
ggF, VBF, $WH + ZH$, $t\bar{t}H + tH$	$H \to \mu\mu$	Sec. 3.3	140	80
WH, ZH	$H \to b\bar{b}$	[3]	140	80
ggF, VBF, $WH + ZH$, $t\bar{t}H + tH$	$H \to \tau\tau$	[4]	140	36
ggF, VBF, $WH + ZH$, $t\bar{t}H + tH$	$H \to ZZ$	[2]	80	80
ggF, VBF	$H \to WW$	[2]	36	36
$t\bar{t}H + tH$	$H \to b\bar{b}$	[2]	36	36
$t\bar{t}H + tH$	$H \to WW, ZZ\ \tau\tau$	[2]	36	36

The projected measurement of the Higgs boson coupling strength scale factors is implemented with the κ-framework. In the combination, the strength parameters for the tree-level couplings to top quark (κ_t), bottom quark (κ_b), tau-lepton (κ_τ), muon (κ_μ), and weak bosons (κ_Z and κ_W), as well as the strength parameters for the three loop-induced effective couplings, namely, the Higgs-gluon coupling (κ_g), the Higgs-photon coupling (κ_γ), and the Higgs-Z-photon coupling ($\kappa_{Z\gamma}$), are free parameters to be simultaneously determined by the combined fit. The coupling for the $gg \to ZH$ process κ_{ggZH} is parameterised as a function of κ_Z and κ_t.

The results are summarised in Figure 7. For consistency with Ref. [2], the scale factor of the charm quark coupling strength κ_c is assumed to be equal to κ_t, in spite of the inclusion in the combination of the dedicated $VH, H \to c\bar{c}$ measurement. The results with κ_c determined as an independent free parameter are documented in Appendix B. In general, ATLAS measurements will be able to constrain the coupling strength scale factors to a typical precision of 2–4%, and overall the expected precision is improved with respect to the projection reported in Ref. [2], particularly for κ_μ and $\kappa_{Z\gamma}$.

The precision of the scale factors for the strengths of the Higgs boson couplings to photons, weak bosons (W and Z), gluons, and elementary fermions of the third generation (t, b, τ) will be limited by theory

uncertainties, while those to muons and to $Z\gamma$ will be limited by the amount of collected data. It should be noted that a significant contribution to the theory uncertainties in the coupling strength scale factors arises from the limited precision of the calculations of the expected SM Higgs boson production rates. These uncertainties will not affect the experimental determination of the Higgs boson cross sections times branching ratios.

With respect to the previous extrapolations in Ref. [2], the projected uncertainties in the coupling strength scale factors are reduced by 7%–29% depending on the coupling, with the exception of κ_Z. For the latter a 4% worse constraint is expected, due to the revised signal modelling uncertainty treatment recommended by the theory community in the $H \to b\bar{b}$ analysis used for this study compared to that used for the previous one.

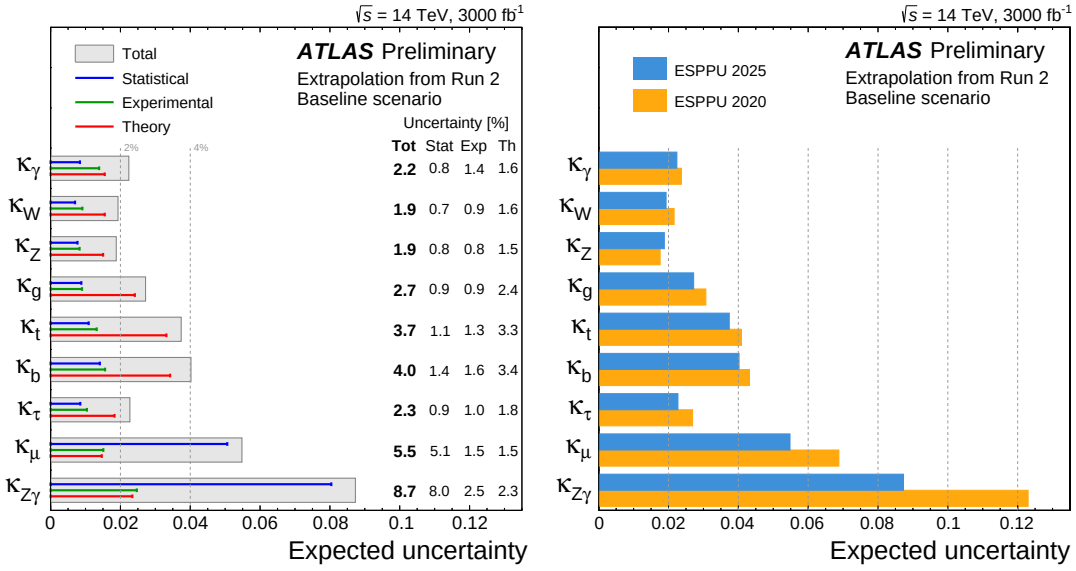

(a) (b)

Figure 7: (a) The projected uncertainty of the combined coupling strength scale factor measurements with 3000 fb^{-1} of pp collisions under the *baseline* systematic uncertainty scenario. (b) Comparison between the results in this note prepared for European Strategy for Particle Physics Update in 2025 (ESPPU 2025) and the previous projection prepared for European Strategy for Particle Physics Update in 2020 (ESPPU 2020) [2].

In order to remove the assumption on the Higgs boson total width, and also to cancel out common systematic uncertainties such as those in the luminosity measurement, the projected measurement of ratios of the Higgs boson coupling strength scale factors is also provided. A reference parameter that represents the high-precision $gg \to H \to ZZ$ rate measurement, $\kappa_{gZ} \equiv \kappa_g\kappa_Z/\kappa_H$, is first introduced. The rates in the other channels, $\sigma_i \times \mathcal{B}(H \to f) = \frac{\kappa_i^2\kappa_f^2}{\kappa_H^2}\sigma_i^{\mathrm{SM}} \times \mathcal{B}^{\mathrm{SM}}(H \to f)$, are then reparameterised in terms of products of κ_{gZ} and of a series of ratios between coupling strength scale factors, defined as $\lambda_{XY} \equiv \kappa_X/\kappa_Y$. The results are summarised in Figure 8. The scale factor related to the charm quark coupling strength κ_c is again assumed to be equal to κ_t in this model. The results with κ_c introduced as an independent free parameter are documented in Appendix B.

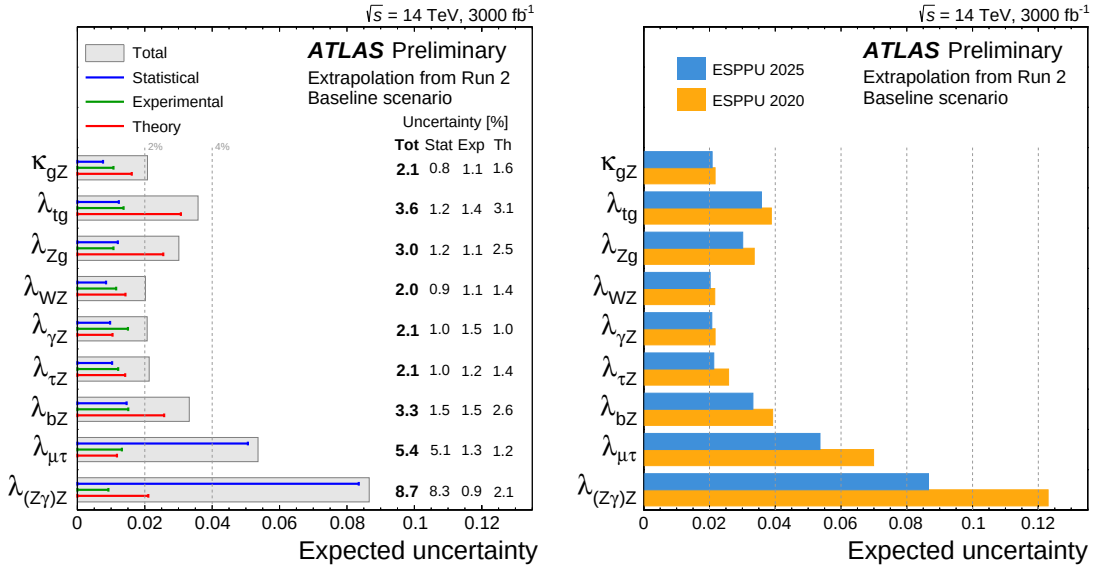

Figure 8: (a) The projected uncertainty of the combined measurements of ratios of coupling strength scale factors with 3000 fb^{-1} of pp collisions under the *baseline* systematic uncertainty scenario. (b) Comparison between the results in this note prepared for European Strategy for Particle Physics Update in 2025 (ESPPU 2025) and the previous projection prepared for European Strategy for Particle Physics Update in 2020 (ESPPU 2020) [2].

4 Conclusion

Understanding the mechanism behind electroweak symmetry breaking and the generation of mass for elementary particles remains a top priority for the future of particle physics. The high-luminosity upgrade of the LHC will provide an exceptional opportunity to explore these phenomena through highly precise and comprehensive measurements of the Higgs boson properties.

This note updates previous projections for Higgs boson measurements in the $H \to \gamma\gamma$, $Z\gamma$ and $\mu\mu$ final states with the ATLAS detector at the HL-LHC, in various scenarios of integrated luminosities and systematic uncertainties. The results are based on extrapolations from the latest published results obtained by the ATLAS Collaboration analysing 140 fb^{-1} of pp collisions at $\sqrt{s}$ = 13 TeV collected in the LHC Run 2, and supersede those of a previous extrapolation [2] based on older publications relying on partial Run 2 datasets.

In the baseline uncertainty scenario, for the nominal integrated luminosity of 3000 fb^{-1} for a single HL-LHC experiment, Higgs boson production cross sections measured in the $H \to \gamma\gamma$, $H \to Z\gamma$, and $H \to \mu\mu$ channels are expected to be determined with an uncertainty that is typically 20% better than in previous extrapolations, showcasing impact from improved analysis techniques developed for the publications based on the full Run 2 dataset compared to those used for the projections of Ref. [2]. A highly granular measurement of Higgs boson production cross sections in simplified fiducial volumes, differential in properties such as Higgs boson transverse momentum or number of hadronic jets produced in the same events, will be possible with typical uncertainties between 5% and 20% using $H \to \gamma\gamma$ decays. These could be translated into constraints of the top Yukawa coupling or the effective Higgs boson coupling to photons or to gluons with few % uncertainty, when all other coupling strengths are fixed to their SM values. Rare Higgs boson decay channels such as $H \to \mu\mu$ and $H \to Z\gamma$ could be observed with large statistical significance, paving the way for determining the muon Yukawa coupling and the effective Higgs

to $Z\gamma$ coupling to better than 10% precision. A lower integrated luminosity of 2000 fb^{-1} would worsen the precision of most of the measurements in the baseline uncertainty scenario by about 20%, with smaller impact (8–15%) on measurements on ggF and VBF production-mode cross sections in $H \to \gamma\gamma$ where the impact of systematic uncertainties is not negligible.

Combining these predictions with recent updates of ATLAS extrapolations of the VH, $H \to b\bar{b}$ [3] and $H \to \tau\tau$ [4] measurements and those of Ref. [2] for other Higgs boson production and decay channels, the expected uncertainties in the Higgs boson coupling strength scale factors in the baseline uncertainty scenario for 3000 fb^{-1} are expected to vary between 1.9% (κ_W, κ_Z) and 8.7% ($\kappa_{Z\gamma}$). Uncertainties in the $gg \to H \to ZZ$ rate scale factor and in ratios of coupling strength scale factors vary between 2.1% and 8.7%.

Appendix

A $H \to \gamma\gamma$ and $H \to Z\gamma$

While the input $H \to \gamma\gamma$ measurement used in this note is able to simultaneously constrain more production modes than the one used in Ref. [2], a merged version of the production mode cross section measurements, as shown in Figure 9, have also been provided for fair comparison with the latter. At 3000 fb^{-1} with the *baseline* systematic uncertainty scenario, the updated $H \to \gamma\gamma$ measurement provides basically the same precision for ggF cross section measurement with respect to Ref. [2], while for VBF, VH, and $t\bar{t}H + tH$ the improvements in precision vary between 15% and 27%.

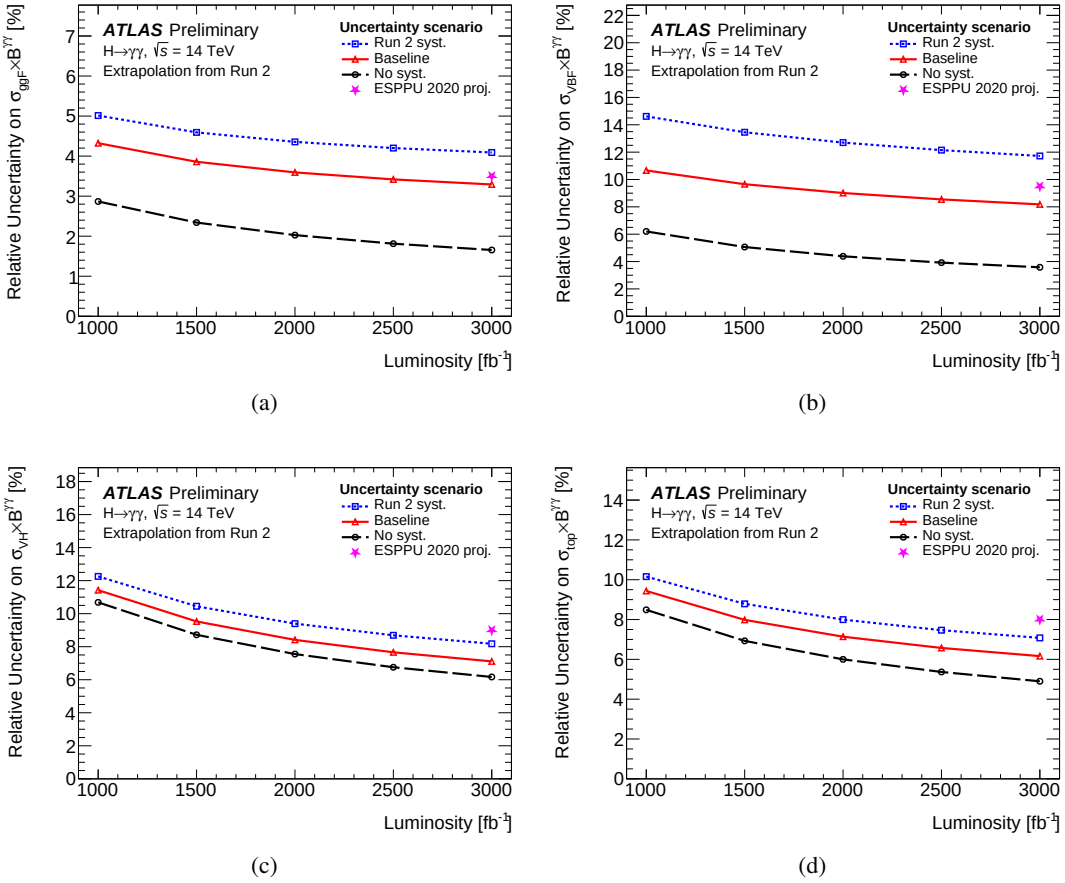

Figure 9: The projected uncertainties on the cross sections of SM (a) ggF, (b) VBF, (c) VH (WH and ZH), and (d) combined $t\bar{t}H$ and tH processes measured in the $H \to \gamma\gamma$ channel by the ATLAS experiment with different integrated luminosities. Three systematic uncertainty scenarios as defined in the text, namely *Run 2* (blue open squares), *baseline* (red open triangles), and *no systematic uncertainties* (black open circles), have been considered. The prediction of the previous projection prepared for European Strategy for Particle Physics Update in 2020 (ESPPU 2020) [2] in a scenario (S2) similar to the *baseline* one for an integrated luminosity of 3000 fb^{-1} is also shown (magenta star).

The projected total uncertainties in the Higgs boson production cross section measurements from the

$H \to \gamma\gamma$ channel at an integrated luminosity of 3000 fb^{-1} have been decomposed into statistical and systematic components as shown in Table 4. The systematic uncertainty is evaluated as the quadratic difference between the total uncertainty and the statistical uncertainty (i.e. *no systematic uncertainties* scenario), for both the *Run 2* and the *baseline* scenarios.

Table 4: The projected relative uncertainties on the cross sections of SM ggF, VBF, WH, ZH, $t\bar{t}H$, and tH processes measured in the $H \to \gamma\gamma$ channel by the ATLAS experiment for an integrated luminosity equal to 3000 fb^{-1}. The *Run 2* and *baseline* systematic uncertainty scenarios are as defined in the text.

Process	Statistical uncertainty	Systematic uncertainty	
		Run 2	*Baseline*
ggF	±2%	±4%	±3%
VBF	±4%	±11%	±7%
WH	±9%	±5%	±3%
ZH	±13%	±9%	±5%
$t\bar{t}H$	±6%	±5%	±4%
tH	±53%	±48%	±12%

To estimate the expected uncertainties when combining two experiments (ATLAS and CMS) with datasets of the same size and similar performance, the $H \to \gamma\gamma$ and $H \to Z\gamma$ analyses have been extrapolated to integrated luminosities as high as 6000 fb^{-1}. A similar study has not been performed for the $H \to \mu\mu$ channel, where the better momentum resolution of the CMS experiment made possible by its larger magnetic field leads to better sensitivity to $H \to \mu\mu$ decays compared to ATLAS. The main results for the $H \to \gamma\gamma$ and $H \to Z\gamma$ analyses for integrated luminosities up to 6000 fb^{-1} are shown in Figures 10, 11 and 12.

For the $H \to Z\gamma$ measurement, that is statistically limited, the uncertainties in the *baseline* scenario improve by about 30% when doubling the integrated luminosity (i.e. from a combination with results with similar precision from CMS). The expected signal strength (effective coupling strength scale factor) precision with a total integrated luminosity of 6000 fb^{-1} is 12% (6%).

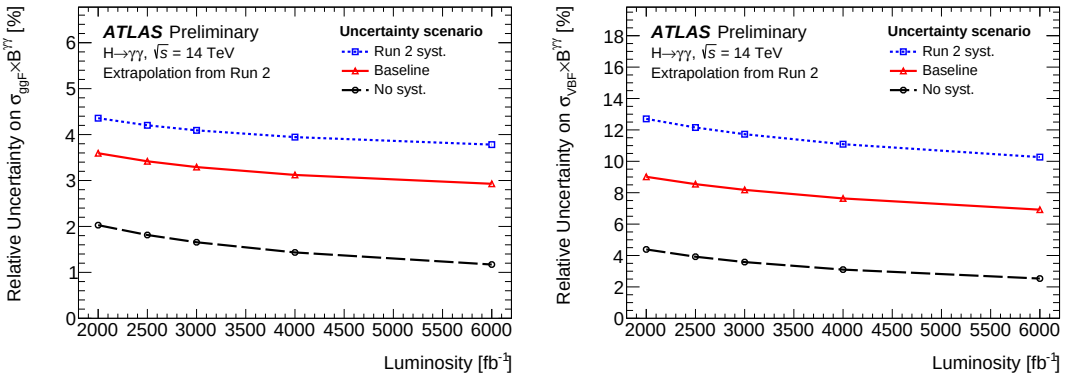

(a)

(b)

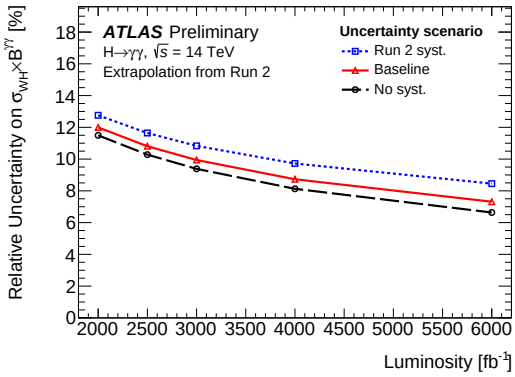

(c)

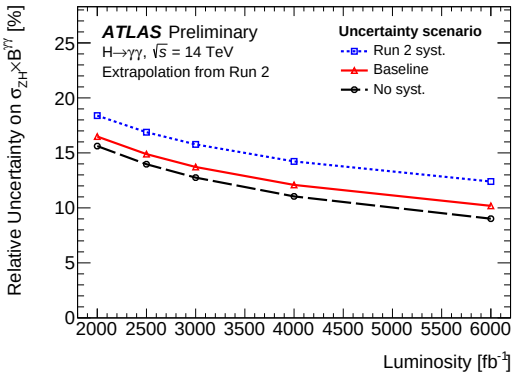

(d)

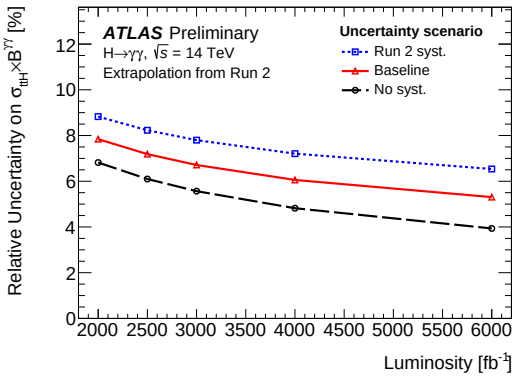

(e)

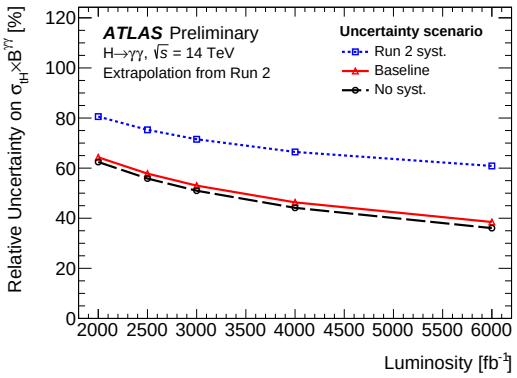

(f)

Figure 10: The projected uncertainties on the cross sections of SM (a) ggF, (b) VBF, (c) WH, (d) ZH, (e) $t\bar{t}H$, and (f) tH processes measured in the $H \to \gamma\gamma$ channel by the ATLAS experiment for integrated luminosities between 2000 and 6000 fb^{-1}. Three systematic uncertainty scenarios as defined in the text, namely *Run 2*, *baseline*, and *no systematic uncertainties*, have been considered. The extrapolation to 6000 fb^{-1} is provided as an approximate to the combined ATLAS and CMS result.

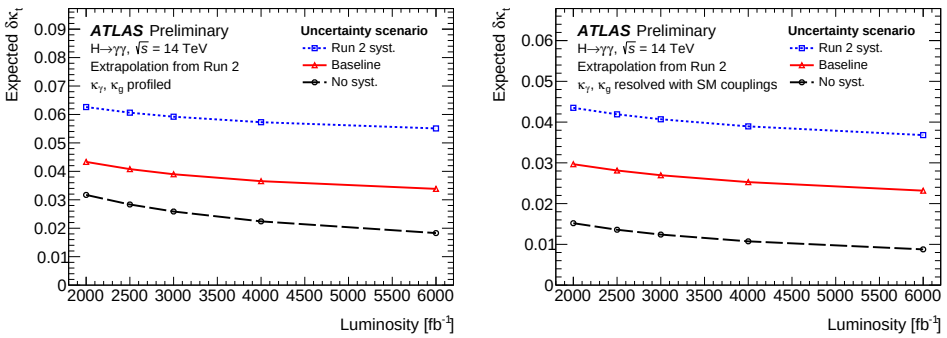

(a) (b)

Figure 11: The projected uncertainty in the top-Higgs Yukawa coupling strength scale factor κ_t measured in the $H \to \gamma\gamma$ channel by the ATLAS experiment for integrated luminosities between 2000 and 6000 fb^{-1}. The measurement is performed either (a) using only tree-level constraint provided by the $t\bar{t}H$ and tH production modes, or (b) also including loop-induced constraints from ggF and $H \to \gamma\gamma$. Other coupling strength scale factors are fixed at SM values. Three systematic uncertainty scenarios as defined in the text, namely *Run 2*, *baseline*, and *no systematic uncertainties*, have been considered. The extrapolation to 6000 fb^{-1} is provided as an approximate to the combined ATLAS and CMS result.

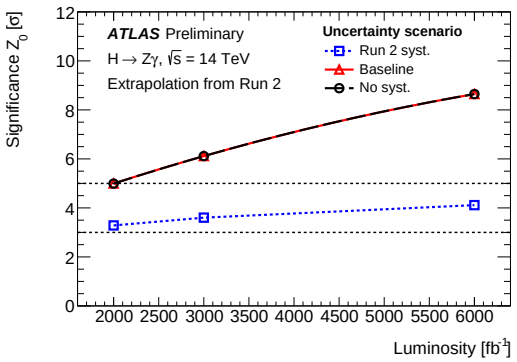

(a)

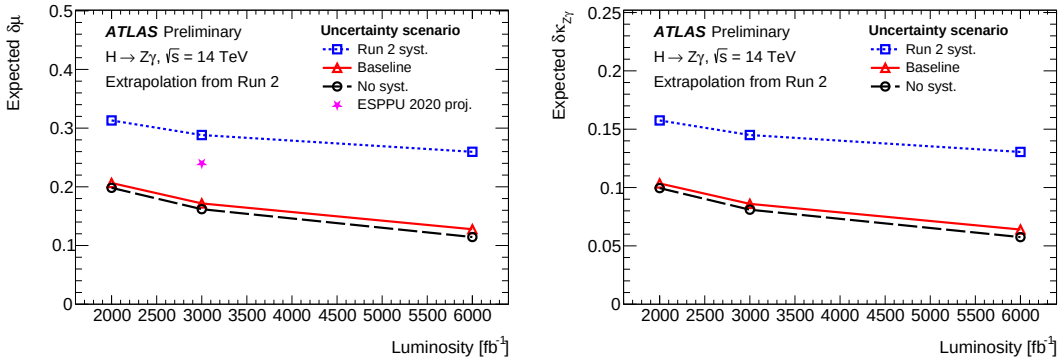

(b) (c)

Figure 12: The projected (a) significance Z_0, (b) signal strength uncertainty $\delta\mu$, and (c) coupling strength scale factor uncertainty $\delta\kappa_{Z\gamma}$ of a SM $H \to Z\gamma$ signal measured by the ATLAS experiment with integrated luminosities between 2000 and 6000 fb^{-1}. Three systematic uncertainty scenarios as defined in the text, namely *Run 2* (blue open squares), *baseline* (red open triangles), and *no systematic uncertainties* (black open circles), have been considered. The prediction of the previous projection prepared for European Strategy for Particle Physics Update 2020 (ESPPU 2020) [2] in a scenario (S2) similar to the *baseline* one for an integrated luminosity of 3000 fb^{-1} is also shown (magenta star). The extrapolation to 6000 fb^{-1} is provided as an approximate to the combined ATLAS and CMS result.

B Combination

The combined fits of the coupling strength scale factors and of their ratios have been performed in a different parameterisation configuration where κ_c is introduced as a free parameter instead of being equated to κ_t. The results are summarised in Figure 13.

In the projection for coupling strengths shown in Figure 13(a), the 95% confidence level upper limit for κ_c is 1.8, and the precision of other coupling strength scale factor measurements decreases compared with results shown in Figure 7 (a) due to the extra degree of freedom introduced by κ_c in the fit. The precision of κ_μ and $\kappa_{Z\gamma}$ are degraded only by 2% and 4%, respectively, as their uncertainty is dominated by statistical uncertainty from the $H \to \mu\mu$ and $H \to Z\gamma$ measurements. For other couplings, the degradation is in general larger: 8% for couplings to third generation quarks κ_t and κ_b, 17% for coupling to tau lepton κ_τ, 26% for couplings to weak bosons κ_W and κ_Z, 15% for effective coupling to gluon κ_g, and 22% for effective coupling to photon κ_γ.

In the projection for the ratios of coupling strengths shown in Figure 13(b), on the other hand, due to the removal of the assumption on the Higgs boson total width and also the marginal contribution to other coupling strengths from the VH, $H \to c\bar{c}$ projection, the projected precision of measurements for parameters that are already in Figure 8 is basically unchanged. The ratio $\lambda_{cb} \equiv \kappa_c/\kappa_b$ is expected to be constrained to be below 1.8 at 95% confidence level.

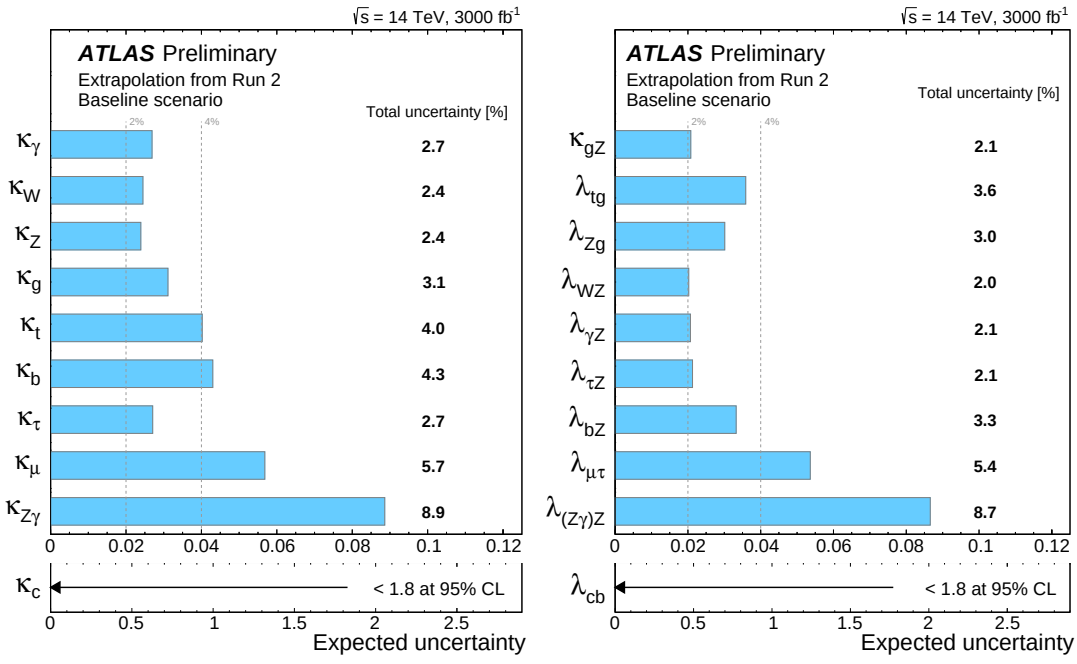

(a) (b)

Figure 13: The projected uncertainty of the combined measurements of (a) coupling strength scale factors and (b) their ratios with 3000 fb^{-1} of pp collisions under the baseline systematic uncertainty scenario. In this fit κ_c is introduced as an independent free parameter in the fit. Due to the limited precision, only 95% confidence level upper limit is reported for κ_c and λ_{cb}. For other coupling strength scale factors and their ratios the 68% confidence intervals are reported instead.

References

[1] A. Dainese et al., *Report on the Physics at the HL-LHC, and Perspectives for the HE-LHC*, tech. rep., 2019, URL: https://cds.cern.ch/record/2703572 (cit. on p. 2).

[2] ATLAS Collaboration, *Projections for measurements of Higgs boson cross sections, branching ratios, coupling parameters and mass with the ATLAS detector at the HL-LHC*, ATL-PHYS-PUB-2018-054, 2018, URL: https://cds.cern.ch/record/2652762 (cit. on pp. 2–5, 9–16, 20).

[3] ATLAS Collaboration, *Expected sensitivity of the ATLAS experiment to $H \to b\bar{b}$ and $H \to c\bar{c}$ decays in the VH production mode at the High Luminosity LHC*, ATL-PHYS-PUB-2025-012, 2025, URL: https://cds.cern.ch/record/2927842 (cit. on pp. 3, 11, 12, 15).

[4] ATLAS Collaboration, *Projection of $H \to \tau\tau$ cross-section measurement results to the HL-LHC*, ATL-PHYS-PUB-2022-003, 2022, URL: https://cds.cern.ch/record/2801396 (cit. on pp. 3, 11, 12, 15).

[5] ATLAS Collaboration, *Expected performance of the ATLAS detector at the High-Luminosity LHC*, ATL-PHYS-PUB-2019-005, 2019, URL: https://cds.cern.ch/record/2655304 (cit. on pp. 3, 4).

[6] ATLAS Collaboration, *Expected tracking and related performance with the updated ATLAS Inner Tracker layout at the High-Luminosity LHC*, ATL-PHYS-PUB-2021-024, 2021, URL: https://cds.cern.ch/record/2776651 (cit. on pp. 3, 4).

[7] ATLAS Collaboration, *ATLAS Inner Tracker Pixel Detector: Technical Design Report*, ATLAS-TDR-030; CERN-LHCC-2017-021, 2017, URL: https://cds.cern.ch/record/2285585 (cit. on p. 3).

[8] D. de Florian et al., *Handbook of LHC Higgs Cross Sections: 4. Deciphering the Nature of the Higgs Sector*, **2/2017** (2016), arXiv: 1610.07922 [hep-ph] (cit. on pp. 3, 4, 9).

[9] J. R. Andersen et al., *Handbook of LHC Higgs Cross Sections: 3. Higgs Properties*, (2013), arXiv: 1307.1347 [hep-ph] (cit. on pp. 3, 4).

[10] ATLAS Collaboration, *Measurement of the properties of Higgs boson production at $\sqrt{s} = 13$ TeV in the $H \to \gamma\gamma$ channel using $139\,fb^{-1}$ of pp collision data with the ATLAS experiment*, JHEP **07** (2023) 088, arXiv: 2207.00348 [hep-ex] (cit. on pp. 3, 5).

[11] ATLAS Collaboration, *A search for the $Z\gamma$ decay mode of the Higgs boson in pp collisions at $\sqrt{s} = 13$ TeV with the ATLAS detector*, Phys. Lett. B **809** (2020) 135754, arXiv: 2005.05382 [hep-ex] (cit. on pp. 3, 9, 10).

[12] ATLAS Collaboration, *A search for the dimuon decay of the Standard Model Higgs boson with the ATLAS detector*, Phys. Lett. B **812** (2021) 135980, arXiv: 2007.07830 [hep-ex] (cit. on pp. 3, 10).

[13] ATLAS and CMS Collaborations, *Snowmass White Paper Contribution: Physics with the Phase-2 ATLAS and CMS Detectors*, ATL-PHYS-PUB-2022-018, CMS PAS FTR-22-001, 2022, URL: https://cds.cern.ch/record/2805993 (cit. on p. 4).

[14] ATLAS Collaboration,
Luminosity determination in pp collisions at $\sqrt{s} = 13$ TeV using the ATLAS detector at the LHC,
Eur. Phys. J. C **83** (2023) 982, arXiv: 2212.09379 [hep-ex] (cit. on p. 5).

[15] ATLAS Collaboration,
Electron and photon energy calibration with the ATLAS detector using LHC Run 2 data,
JINST **19** (2024) P02009, arXiv: 2309.05471 [hep-ex] (cit. on p. 5).

[16] D. de Florian et al.,
Handbook of LHC Higgs Cross Sections: 4. Deciphering the Nature of the Higgs Sector, (2017),
arXiv: 1610.07922 [hep-ph] (cit. on p. 5).

[17] ATLAS and CMS Collaborations,
Evidence for the Higgs Boson Decay to a Z Boson and a Photon at the LHC,
Phys. Rev. Lett. **132** (2024) 021803, arXiv: 2309.03501 [hep-ex] (cit. on p. 9).

[18] ATLAS Collaboration, *Searches for the $Z\gamma$ decay mode of the Higgs boson and for new high-mass resonances in pp collisions at $\sqrt{s} = 13$ TeV with the ATLAS detector*, JHEP **10** (2017) 112,
arXiv: 1708.00212 [hep-ex] (cit. on p. 10).

[19] ATLAS Collaboration, *A search for the rare decay of the Standard Model Higgs boson to dimuons in pp collisions at $\sqrt{s} = 13$ TeV with the ATLAS detector*, ATLAS-CONF-2018-026, 2018,
URL: https://cds.cern.ch/record/2628763 (cit. on p. 11).